

# Surface Roughness Estimation for Reproducing Appearance of Glossy Object Surfaces

Shoji Tominaga; Norwegian University of Science and Technology, Gjøvik, Norway / Nagano University, Ueda, Japan  
Motonori Doi; Osaka Electro-Communication University, Neyagawa, Japan

## Abstract

*We consider the estimation of surface roughness to reproduce the appearance of objects with smooth and glossy surfaces such as lacquerware and plastic objects. Two methods comprising measurement-based and image-based roughness are used for estimation. First, a laser scanning system is used to measure the microscopic surface height of the target object and calculate the surface normal vectors at every grid point from the height information. The surface roughness is then calculated as the 2D deviation of the surface normal vectors. Next, the Beckmann roughness parameter is then estimated using a high-dynamic-range (HDR) image captured from a flat surface of the target material. The specular lobe is approximated using the Beckmann distribution function with a surface roughness parameter. Furthermore, images are rendered to reproduce the surface appearance and confirm the reliability of the estimated roughness parameters. We study the relationship between the measurement- and image-based roughness and find a linear relationship between them. The Beckmann roughness parameter required for image rendering is predicted from the measured roughness.*

## Introduction

Lacquerware refers to objects covered with lacquer. Lacquerware includes tableware, containers, furniture, daily necessities, and various small and large objects carried by people. East Asian countries such as Japan, China, and Korea have long traditions of lacquer work that date back to several thousands of years [1]. The best-known lacquer is a urushiol-based lacquer common in East Asia obtained from the dried sap of *Toxicodendron vernicifluum* [2].

Most lacquerware is handmade. Every lacquerware object made with the traditional technique, which has been in use for more than 900 years, is produced using natural wood and urushi lacquer. However, the use of traditional lacquerware has decreased recently because of the increase in cheaper plastic-based lacquerware-like objects. Plastic lacquerware-like objects are so well-made that it is difficult to judge whether an object is plastic or real lacquerware through a casual glance.

Figure 1 shows a comparison between two red sake cups. The left cup is a real lacquer cup and the right one is a synthetic plastic cup. Both cups have strong gloss and radiance and a beautiful surface appearance. Unlike natural lacquerware handmade by craftspeople, most synthetic objects are mass-produced through molding by pouring plastic into a mold.

In this study, we analyze the surface characteristics of lacquerware and plastic objects to reconstruct the appearance of such strongly glossy objects. The overall appearance of three-dimensional (3D) objects results from a combination of the chromatic factor of the surface spectral reflectance and geometric

factors such as the surface shape and texture. It is however not possible to distinguish between real lacquerware and plastic objects based only on their spectral reflectance and 3D surface shapes. We believe that the appearance of the surfaces is also affected by the surface microstructure.

The surface roughness is a measure of the microscopic surface structure. It is quantified by the height deviation along the vertical direction relative to that in the surface shape of an object with an ideal surface. A variety of methods to measure the surface roughness have been proposed for industrial surface inspection [3]. The International Organization for Standardization (ISO) specifies the well-known standard roughness parameter,  $R_a$ , in ISO 4287:1997. However,  $R_a$  does not necessarily match the perceived appearance of the surface roughness on an object. Instead, the perceived appearance of the surface roughness is correlated with the deviation of the surface normal vectors. Ohtsuki et al. [4] analyzed the surface roughness of human skin, and Oren and Nayar [5] proposed a reflection model for rough surfaces such as concrete and sand in which the surface normals of the surfaces are described using 1D Gaussian distributions.

So far, function models that use roughness as a parameter, such as the Beckmann function [6], have often been used to render the realistic appearance of objects [7]-[11]. However, such a roughness is merely a roughness parameter in a mathematical model and does not necessarily represent the actual physical roughness.

In the present study, we define a 2D surface roughness for a glossy smooth object surface, which differs from that for a matte object. The surface layers of lacquerware and plastic objects are optically regarded as inhomogeneous dielectric materials. Their reflection behavior can be described using a dichromatic reflection model in which the spectral composition of light reflected from the object surface is decomposed into two additive components comprising the diffuse (body) reflection and specular (interface) reflection components [12-14]. The specular profile, which represents the reflection distribution around a specular highlight, plays an important role in determining the appearance of a material [15].

We first use a laser scanning system to measure the microscopic surface height of the target object and calculate the surface normal vectors at every grid point using the height information. The surface roughness is defined based on the 2D deviation of the surface normals.

We then estimate the roughness parameter from camera images of the same target object. The shape of the specular lobe generated by dichromatic reflection has a significant dependence on the surface roughness. The specular lobe is approximated using the Beckmann distribution function with a surface roughness parameter, which is estimated from the captured high-dynamic-range (HDR) image of a flat surface of the target material.

Furthermore, we study the relationship between the surface roughness obtained by directly measuring the object surface, which we call the measurement-based roughness, and the surface roughness estimated from the camera data, which we call the image-based roughness, and find that there is a linear relationship between the two types of roughness. Thus, the roughness parameter required for image rendering can be predicted from the roughness obtained using surface measurements.



Figure 1. Comparison of two red sake cups. The left cup is a real lacquer cup and the right one is a synthetic plastic cup.

### Measurement-Based Roughness Estimation

The laser scanning system was used to obtain the precise surface height information of the target objects. The system consists of an XY stage and a laser confocal displacement meter (Keyence, Model LT8110). The surface of the object was scanned with high accuracy at a resolution of  $5 \mu\text{m}$ . The advantage of this measurement system is that unlike a camera system, there is no lens distortion owing to the direct measurement of the surface.

The surface heights at tiny rectangular areas on the surface of the target object, each with the dimensions of  $1 \text{ mm} \times 0.5 \text{ mm}$ , were measured with a pitch of  $5 \mu\text{m}$ , and the entire height profile was obtained over  $201 \times 101$  grid points. Because the target surface was not perfectly flat, the base surface was determined via smoothing using a moving average and the height deviation was calculated as the difference between the measured and base heights. The measurements may vary depending on the location of the cutout. However, since it is physically difficult to measure a wide area, we chose to measure such a small area.

We measured the surfaces of different examples of real lacquerware and opaque plastic objects. Figure 2 shows the measured height deviation distributions of the surfaces using meshes where panels (a) and (b) show the measurement results for the real lacquerware and plastic objects, respectively. The unit of the z-axis scale is mm.

The MATLAB function `pcnormals` was used to estimate the surface normal vectors from the height data. In this function, the six neighboring points to each point are used for local plane fitting to determine the normal vector at the point [16]. The 3D distributions of the normal vectors suggest that the surface features of the lacquerware and plastic objects are significantly different. As an example, Figure 3 shows the differences in the 3D distributions of the surface normals between lacquerware and plastic, where red and black represent the red urushi flat plate lacquerware and black acrylic flat plate plastic object, respectively. The surface normals of the lacquerware are widely distributed whereas those of the plastic object are mostly oriented toward the zenith.

Figure 4 shows images shaded using the surface normals obtained at the grid points over the surface of each object in Figure 2. The illumination was assumed to be incident at  $45^\circ$ . A comparison

of the two sets of images in Figure 4(a) and (b) shows that the surfaces of the real lacquerware are rougher than those of the plastic objects. The surface roughness  $R$  is defined as the deviation from the average surface normal vector as follows:

Let  $N$  be the total number of surface normal data points. The surface normal vector  $\mathbf{w}_i$  ( $i=1, 2, \dots, N$ ) at the  $i$ th point and the averaged vector  $\mathbf{w}_0$  are described using 3D column vectors as

$$\mathbf{w}_i = \begin{bmatrix} x_i \\ y_i \\ z_i \end{bmatrix} \quad (i = 1, 2, \dots, N), \quad (1)$$

$$\mathbf{w}_0 = \begin{bmatrix} x_0 \\ y_0 \\ z_0 \end{bmatrix} = \frac{1}{N} \sum_{i=1}^N \mathbf{w}_i, \quad (2)$$

where

$$\|\mathbf{w}_i\| = \|\mathbf{w}_0\| = 1. \quad (3)$$

We define the autocorrelation matrix  $\mathbf{T}$  and the scalar  $J$  as

$$\mathbf{T} = \frac{1}{N} \sum_{i=1}^N \mathbf{w}_i \mathbf{w}_i^t, \quad (4)$$

$$J = 1 - \mathbf{w}_0^t \mathbf{T} \mathbf{w}_0, \quad (5)$$

where the superscript  $t$  denotes matrix transposition. We then have

$$\begin{aligned} J &= \frac{1}{N} \sum_{i=1}^N (1 - \mathbf{w}_0^t \mathbf{w}_i \mathbf{w}_i^t \mathbf{w}_0) \\ &= \frac{1}{N} \sum_{i=1}^N (1 - (\mathbf{w}_0^t \mathbf{w}_i)^2) \end{aligned} \quad (6)$$

Owing to the constraints in Eq. (3) and the fact that  $\mathbf{w}_0^t \mathbf{w}_i$  is the inner product of  $\mathbf{w}_0$  and  $\mathbf{w}_i$ ,  $\mathbf{w}_0^t \mathbf{w}_i = \cos \theta_i$  where  $\theta_i$  is the angle between  $\mathbf{w}_0$  and  $\mathbf{w}_i$ , as shown in Figure 5. Eq. (6) can thus be rewritten as

$$J = \frac{1}{N} \sum_{i=1}^N (1 - (\cos \theta_i)^2) = \frac{1}{N} \sum_{i=1}^N (\sin \theta_i)^2 \quad (7)$$

where  $\sin \theta_i$  is the length of the perpendicular line drawn from the tip of the vector  $\mathbf{w}_i$  to  $\mathbf{w}_0$  (see Figure 5). That is,  $J$  is the mean of the squares of the lengths of the perpendicular lines drawn from each  $\mathbf{w}_i$  to the average vector  $\mathbf{w}_0$ . Therefore, the square root of  $J$ ,  $\sqrt{J} (\triangleq R)$ , is the standard deviation of the surface normal vectors, that is, the surface roughness  $R$  defined above.

The values of the surface roughness  $R$  were calculated from the normal data of the lacquerware and plastic objects using Eq. (5) and found to be as follows:

For lacquerware,  $R_1=0.294$ ,  $R_2=0.260$ .

For plastic objects,  $R_1=0.0310$ ,  $R_2=0.0631$ .

Thus, even though the surfaces of the lacquerware appear smooth microscopically, they are considerably rougher than the surfaces of the plastic objects.

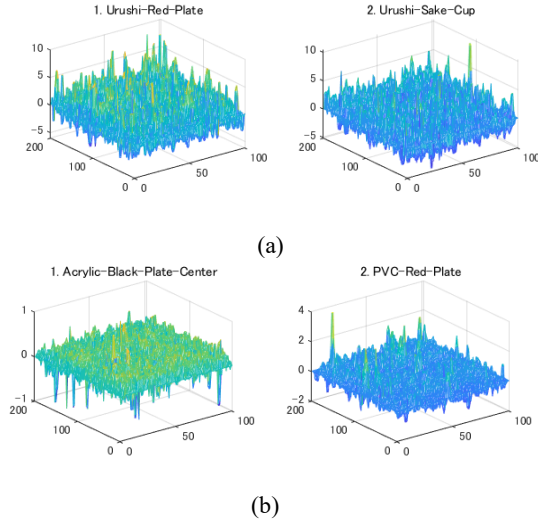


Figure 2. Measured height deviation distributions displayed using meshes: (a) real lacquerware, (b) plastic objects.

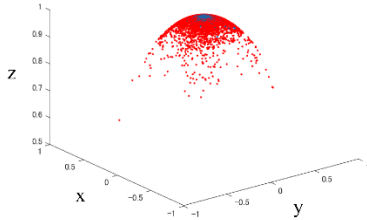


Figure 3. 3D distribution of the surface normals for lacquerware and plastic where red and black represent the lacquerware urushi red plate and the plastic acrylic black plate, respectively.

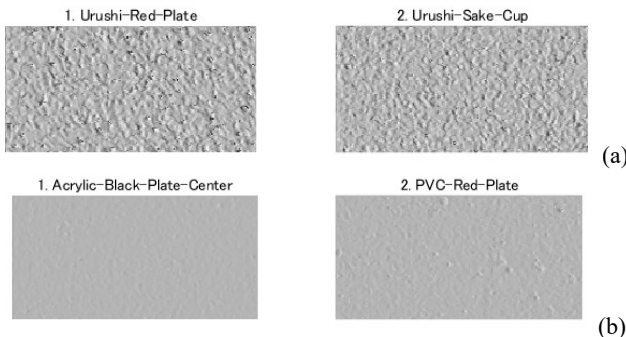


Figure 4. Images shaded using the surface normals at the grid points on each surface in Figure 3 for illumination incident at 45°.

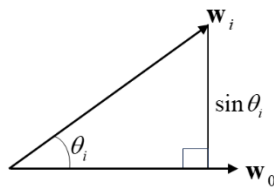


Figure 5. Relationship between surface normal and averaged vectors.

## Image-Based Roughness Parameter Estimation

We estimate the roughness parameter for each object measured using the laser scanning system from camera images of the same object. The specular function of a dielectric material is a mathematical function used to model its specular reflection. This function does not include color (spectral) information but mainly reflects the geometric information of the specular surface, which depends on the surface orientation, illumination, and viewing direction. Therefore, it can accurately represent the appearance of a glossy material using parameters related to its roughness and sharpness.

Consider a simple reflection geometry in which  $\mathbf{N}$  is the surface normal vector,  $\mathbf{L}$  the incident light vector, and  $\mathbf{V}$  the viewing vector. Let  $\mathbf{R}_L$  and  $\mathbf{R}_V$  be  $\mathbf{L}$  and  $\mathbf{V}$  mirrored about  $\mathbf{N}$ , respectively. Specular reflection is observed only within a restricted range of viewing angles. This reflection component is often the strongest along the direction of  $\mathbf{R}_L$  and falls off sharply as the angle  $\theta$  between  $\mathbf{R}_L$  and  $\mathbf{V}$  increases. This rapid falloff is often approximated as

$$f(\theta) = \beta \cos^n \theta \quad (8)$$

where  $\beta$  is a constant representing the specular peak intensity and  $n$  is a measure of the surface roughness. This type of intensity distribution is called the Phong distribution [7]. If the highlight has a pointed peak, a Gaussian distribution can be used to model the sharp falloff as follows:

$$f(\theta) = \beta \exp(-n\theta^2) \quad (9)$$

However, simple specular functions such as the Phong distribution cannot describe the surface specularity of rough surfaces adequately because the constant parameters are unknown. In addition, there is always some surface roughness even if the surface appears smooth. The shape of the specular reflection lobe generated by dichromatic reflection depends significantly on the surface roughness. Rough specular surfaces are idealized as being composed of small planar surface patches called microfacets.

The Beckmann distribution is a physics-based microfacet distribution model [6]. The specular lobe can be approximated using the Beckmann distribution function with a surface roughness parameter  $m$  as

$$f(\varphi) = \left( \frac{1}{m^2 \cos^4 \varphi} \right) \exp\left\{ -\left( \tan \varphi / m \right)^2 \right\}, \quad (10)$$

where  $m$  represents the roughness of the object surface.  $\varphi$  is the angle between  $\mathbf{Q}$  and  $\mathbf{N}$  where  $\mathbf{Q}$  is the vector bisector of  $\mathbf{L}$  and  $\mathbf{V}$ . Compared to the empirical models in Eqs. (8) and (9) above, this function gives the absolute magnitude of the reflectance without the need to introduce arbitrary constants.

To estimate the Beckmann roughness parameter from camera images, we consider a simple measurement setup. Figure 6 shows the capture process for a glossy flat object surface where the light source and camera are placed at a high vertical position and the curve represents the 1D reflection distribution. In this case, the angles  $\varphi$  and  $\theta$  are both equal to the viewing angle. In the actual system we used, the distance between the object and light source (camera) was 1040 mm, and the light source was a small LED. We used a digital single-lens reflex (DSLR) camera (Sony alpha 7C) with a bit depth of 14 bits for each color signal. The camera images

were captured in the lossless SONY-ARW raw image format. The captured images of the object surface include glosses or highlights. Numerous images were captured by changing the shutter speed and then linearly combined to obtain an image without saturation and with the highest dynamic range as a HDR image of the target surface.

Figure 7 shows the HDR images captured from the (a) urushi red plate and (b) acrylic black plate. Relative values were calculated from the captured images based on a white reference standard with a matte surface photographed under the same conditions. Figure 8 shows the corresponding mesh representations of the luminance intensity distributions for (a) and (b). The mesh size is  $512 \times 512$ , and each pixel corresponds to approximately  $0.0246^\circ$ . Assuming that the reflection is symmetric, the 1D profile of the intensity distribution can be fitted to the Beckmann function in Eq. (10). For visual matching of the appearance, fitting in the wider highlight lobe in the glossy HDR images is more significant than fitting in the highlight peak point. Therefore, the inverse gamma correction nonlinear transformation was applied to the pixel intensity values  $I$  as  $Z = I^{1/\gamma}$ , where  $\gamma$  was set to 2.0 as in the previous HDR image analysis [17]. There is no essential difference even if  $\gamma=2.2$  is used. Figure 9 shows the results of least-squares fitting to the Beckmann distribution, where each 1D dimensional distribution is one-dimensional distribution along the X-direction in the 2D distribution of Figure 8. The fitting results are represented as functions of the viewing angle where the black and red curves represent the HDR-measured curve and the fitted Beckmann function, respectively. The roughness parameters are  $m=0.01859$  and  $m=0.002288$  for (a) and (b), respectively. The original measured curve in (b) is almost coincident with the fitted Beckmann distribution.



Figure 6. Image capture setup for a glossy flat object surface.

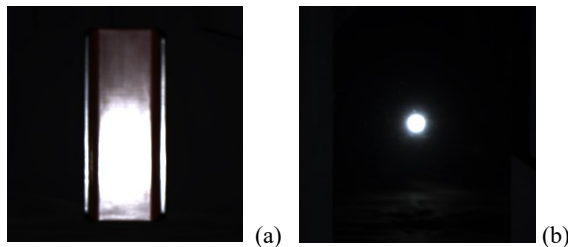


Figure 7. HDR images captured from the (a) urushi red plate and (b) acrylic black plate.

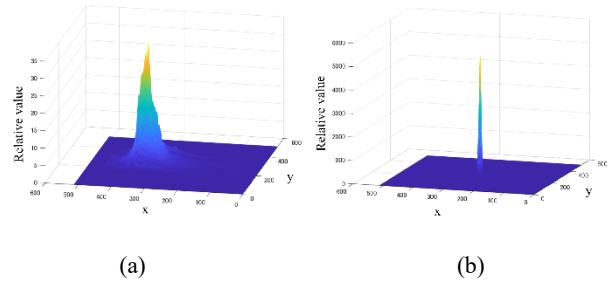


Figure 8. Corresponding mesh representations of the luminance intensity distributions: (a) urushi red plate and (b) acrylic black plate.

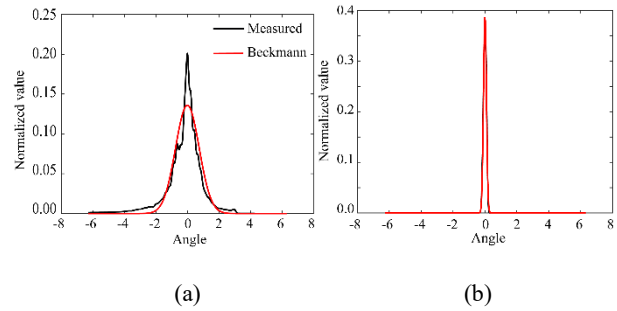


Figure 9. Least-squares fitting results for the Beckmann distribution where the black and red curves represent the HDR measured curve and the fitted Beckmann function, respectively: (a) urushi red plate and (b) acrylic black plate.

## Appearance Reproduction Using Estimated Roughness Parameters

The Cook–Torrance model [8] is used as a reflection model to reproduce the realistic appearance of glossy objects under various conditions. The spectral reflection model for the color signal, which includes the light source and reflectance, is given by

$$C(\mathbf{N}, \mathbf{V}, \mathbf{L}, \lambda) = (\mathbf{N} \cdot \mathbf{L}) S_d(\lambda) E(\lambda) + c F_0 \frac{f(\varphi) G(\mathbf{N}, \mathbf{V}, \mathbf{L})}{(\mathbf{N} \cdot \mathbf{V})(\mathbf{N} \cdot \mathbf{L})} S_p(\lambda) E(\lambda), \quad (11)$$

where the first and second terms in the right hand side represent the diffuse and specular reflection components, respectively,  $c$  is a constant,  $E(\lambda)$  the spectral power distribution of the light source,  $S_d(\lambda)$  the spectral reflectance for the diffuse reflection component,  $S_p(\lambda)$  the spectral reflectance for the specular reflection component,  $F_0$  the Fresnel reflectance at normal incidence,  $f(\varphi)$  the Beckmann distribution function in Eq. (10), and  $G$  the geometric attenuation factor describing self-shadowing due to the microfacets (see [13]).

We used the physical spectral renderer Mitsuba [17] to predict the reflection based on an underlying Monte Carlo simulation. The Cook–Torrance model was implemented in the renderer by Guarnera [15]. The reflectance and illuminance spectral functions were represented in 5 nm intervals within the wavelength range of 400–700 nm. A perspective camera model was used to set the field of view such that the rendered image fitted the acquired image. The location and orientation of the camera and lighting were adjusted to match the actual camera images. An output image with the size of

512 by 512 pixels was spectrally rendered. The 3D shape data of the objects acquired using a 3D scanner were input as OBJ files. The spectral reflectance  $S_d(\lambda)$  and illuminant distribution  $E(\lambda)$  from the target object and the actual light source were measured using a spectral colorimeter and spectral radiometer, respectively. The specular reflectance  $S_p(\lambda)$  was set to 1. The attenuation factor  $G$  could be regarded to 1 (no shadowing) in the usual observation condition for a smoothed surface. The color signal  $C$  obtained at each pixel was converted into the tri-stimulus values XYZ and sRGB.

We first confirm the reliability of the estimated roughness parameters in the rendered images. Figure 10 shows the images of the (a) urushi red plate and (b) acrylic black plate rendered in Mitsuba based on the setup shown in Figure 6. The light source was assumed to be a point light source. The intensity profile around the specular peak was obtained from each rendered image and its distribution compared with those of the original measured intensity and fitted Beckmann distributions. Figure 11 shows a comparison between the specular profiles of the original measured intensities and those of the fitted Beckmann and rendered image intensity distributions. The rendered images reproduce the estimated Beckmann distributions well. In particular, in (b), the three curves are so similar that they are indistinguishable.

It should be noted that it is difficult to estimate the Beckmann roughness parameter for a curved object surface because the estimation method is limited to a flat object surface, as shown in Figure 6. Therefore, we estimated the Beckmann roughness parameter from the measurement-based roughness values obtained using the laser scanning system. The measurement-based roughness  $R$  and the corresponding image-based Beckmann roughness parameter  $m$  were obtained for five flat objects comprising the acrylic black plate, PVC black plate, urushi red plate, urushi black plate, and urushi cover surface.

The calculated correlation coefficient between each  $R$  and  $m$  element pair,  $corr(R, m) = 0.9899$ . This indicates that there is a strong correlation between the measurement-based roughness values and the image-based Beckmann roughness parameters. Therefore, to predict the Beckmann roughness parameters from the measured roughness values, we created a simple linear regression model

$$R = c_0 + c_1 m + \varepsilon, \quad (12)$$

where  $\varepsilon$  is the error term. The coefficients  $c_0$  and  $c_1$  were estimated by least-squares fitting of the data for flat objects as  $c_0 = -6.156e-04$  and  $c_1 = 0.0712$ , respectively. Figure 12 shows the fitting results for the regression line. Note that  $c_0$  is almost zero; therefore, the regression line passes through the origin.

The Beckmann roughness parameters for the lacquer and plastic cups in Figure 1 were hence estimated as  $R_1 = 0.0185$  and  $R_2 = 0.0043$ , respectively. Figures 13(a) and (c) show the images rendered using the estimated values for the surface roughness of the lacquer and plastic cups. The light source was assumed to be directional and illuminating the surface in a direction slightly shifted from the vertical direction of the cup with the same spectral distribution as that of the LED. The image in Figure 13(c) was rendered using the 3D shape of the lacquer cup, but the actual plastic reflectance was used for comparison with the appearance of the

lacquer cup. Figures 13(b) and (d) show the respective actual images for comparison. The appearance in (a) and (b) is slightly different.

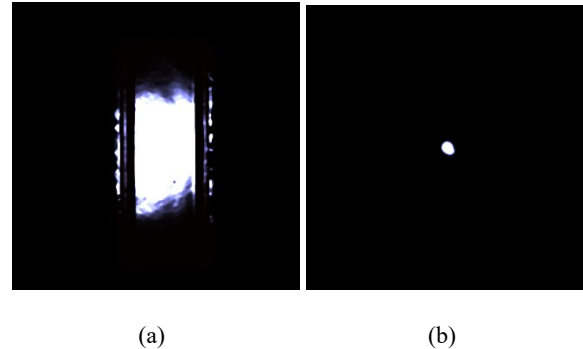


Figure 10. Images of (a) urushi red plate and (b) acrylic black plate rendered by Mitsuba based on the setup in Figure 7.

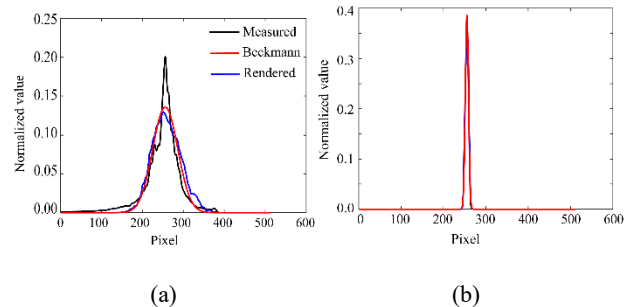


Figure 11. Comparison between the specular profiles of the original measured intensity (black) and the fitted Beckmann (red) and rendered (blue) image intensity distributions: (a) urushi red plate, (b) acrylic black plate.

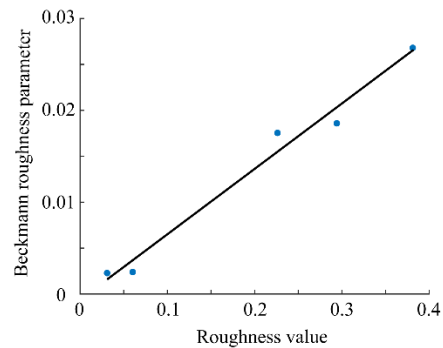
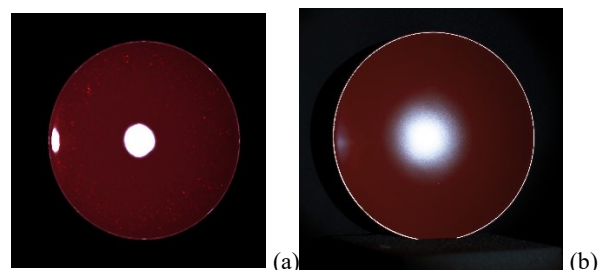
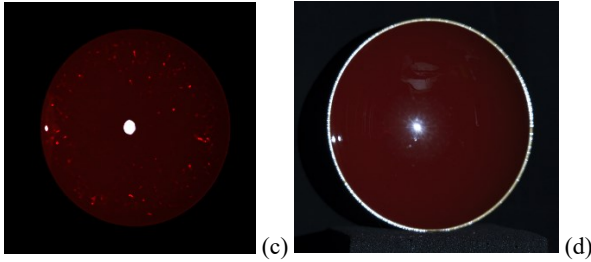


Figure 12. Regression line fitting result for measurement- and image-based roughness.





Figures 13. Images rendered using the estimated values of the surface roughness  $R_1$  and  $R_2$  for the (a) lacquer and (c) plastic cup, and the corresponding actual images (b) and (d) for comparison.

## Conclusions

In this study, we have considered the estimation of surface roughness to reproduce the appearance of smooth and glossy object surfaces such as lacquerware and plastic objects. The surface layer was modeled as an inhomogeneous dielectric material and the light reflection was described using a dichromatic reflection model. We presented two forms of roughness, namely, the measurement-based and the image-based roughness.

We first used a laser scanning system to measure the microscopic surface height of the target object and calculated the surface normal vectors at every grid point from the height information. The surface roughness was then obtained based on the 2D deviation of the surface normal vectors.

We then estimated the roughness parameter from the camera images of the target object. The specular lobe was approximated using the Beckmann distribution function with a surface roughness parameter, which was estimated from the captured HDR image of a flat surface of the target material.

Furthermore, we rendered images to reproduce the surface appearance and confirmed the reliability of the estimated roughness parameters. We studied the relationship between the measurement-based and image-based roughness and found a linear relationship between the two types of roughness. The Beckmann roughness parameter required for image rendering could thus be predicted from the roughness obtained using surface measurements.

Thus, although lacquer and plastic objects look very similar, it is possible to distinguish between them based on the difference in surface roughness. Our future work will involve increasing the number of object samples to demonstrate the generalizability of our finding of a linear relationship between roughness measurements and Beckmann function parameters. Further, we will study the possibility of applying this to other objects than lacquer and plastic objects.

## References

[1] <https://en.wikipedia.org/wiki/Lacquerware> (accessed on 18 June 2024).

- [2] [https://en.wikipedia.org/wiki/Toxicodendron\\_vernicifluum](https://en.wikipedia.org/wiki/Toxicodendron_vernicifluum) (accessed on 18 June 2024).
- [3] M.Q. Shao et al., A review of surface roughness measurements based on laser speckle method, *J. Iron Steel Res. Int.*, Vol. 30, pp. 1897–1915 (2023).
- [4] R. Ohtsuki, T. Sakamaki, and S. Tominaga, Analysis of skin surface roughness by visual assessment and surface measurement, *Optical Review*, Vol.20, No.2, pp.94-101 (2013).
- [5] M. Oren and S. Nayar, Generalization of the Lambertian model and implications for machine vision, *Int. J. Computer Vision*, Vol. 14, pp. 227-251 (1995).
- [6] P. Beckmann and A. Spizzichino, *The Scattering of Electromagnetic Waves from Rough Surfaces*, Pergamon Press, Oxford, 1-33, 70-98 (1961).
- [7] B. T. Phong, “Illumination for computer-generated pictures,” *Comm. ACM*, 18, 311-317 (1975)
- [8] R. L. Cook and K. E. Torrance, A reflection model for computer graphics, *ACM Trans. on Graphics*, Vol. 1, pp. 7-24 (1982)
- [9] M. Ribardière, D. Meneveaux, B. Bringier, and L. Simonot Appearance of interfaced Lambertian microfacets using STD distribution, *Workshop on Material Appearance Modeling*, pp. 1-6 (2017)
- [10] J.H. Lee, A. Jarabo, D.S. Jeon, D. Gutierrez, and M.H. Kim, Practical multiple scattering for rough surfaces, *ACM Trans. Graph.*, Vol.37, No. 6, 275, pp. 1-12 (2018).
- [11] X. Chermain, F. Claux, and S. Mérillou, A microfacet-based BRDF for the accurate and efficient rendering of high-definition specular normal maps, *The Visual Computer*, Vol. 36, pp. 267–277 (2020).
- [12] S. Tominaga and B. Wandell Standard reflectance model and illuminant estimation. *J. Opt. Soc. Am. A.*, Vo. 6, No. 4, pp. 576-584 (1989).
- [13] S. Tominaga, Surface identification using the dichromatic reflection model, *IEEE Trans Pattern Anal. Mach. Intel.*, Vol. 13, No. 7, pp. 658-670 (1991).
- [14] S. Tominaga, Dichromatic reflection models for a variety of materials, *Color Res Appl.*, Vol. 19, No. 4, pp. 277-285 (1994).
- [15] S. Tominaga and G. C. Guarnera, Measuring, modeling, and reproducing material appearance from specular profile, *Proc. Color and Imaging Conference (CIC27)*, pp.279-283 (2019).
- [16] MATLAB pcnormals, <https://jp.mathworks.com/help/vision/ref/pcnormals.html?lang=en>.
- [17] S. Tominaga and T. Horiuchi, High dynamic range image reconstruction from saturated images of metallic objects, *Journal of Imaging*, Vol.10, pp. 1-17 (2024).
- [18] <https://www.mitsuba-renderer.org>.

## Author Biography

Shoji Tominaga received the B.E., M.S., and Ph.D. degrees in electrical engineering from Osaka University, Japan. He was a Professor (2006-2013) and Dean (2011-2013) at Graduate School in Chiba University. He is now an Adjunct Professor, Norwegian University of Science and Technology and also a Visiting Researcher, Nagano University. His research interests include multispectral imaging, and material appearance. He is a Fellow of IEEE, IS&T, SPIE, and OSA